OPEN

Feasibility of Amylin Imaging in Pancreatic Islets with β-Amyloid Imaging Probes

Masashi Yoshimura, Masahiro Ono, Hiroyuki Watanabe, Hiroyuki Kimura & Hideo Saji

Department of Patho-Functional Bioanalysis, Graduate School of Pharmaceutical Sciences, Kyoto University, 46-29 Yoshida Shimoadachi-cho, Sakyo-ku, Kyoto 606-8501, Japan.

Islet amyloid deposition composed of amylin aggregates is regarded as one of the hallmarks of type 2 diabetes mellitus (T2DM). For the diagnosis of T2DM, several nuclear medical imaging probes have been developed. However, there have been no reports regarding the development of imaging probes targeting amylin. In this report, we investigated the feasibility of amylin imaging using [^{125}I]IPBF as one of the model compounds of β-amyloid (Aβ) imaging probes. In in vitro experiments, [^{125}I]IPBF exhibited high binding affinity for amylin aggregates (K_d = 8.31 nM). Moreover, autoradiographic images showed that [^{125}I]IPBF specifically bound to islet amyloid composed of amylin. These results suggest the potential application of Aβ imaging probes to amylin imaging. In addition, [^{125}I]IPBF is one of the promising lead compounds for amylin imaging, and further structural optimization based on [^{125}I]IPBF may lead to useful tracers for the in vivo imaging of islet amyloids in the pancreas.

D iabetes mellitus constitutes one of the most common chronic diseases characterized by hyperglycemia resulting from defects in insulin secretion, insulin action, or both. It was estimated in 2010 that 285 million adults had been diagnosed with diabetes mellitus worldwide, and such patients will have increased to 439 million adults by 2030[1]. Approximately 90% of diabetic patients suffer from type 2 diabetes mellitus (T2DM), known as non-insulin-dependent diabetes mellitus[1]. Currently, the diagnosis of T2DM depends on the blood glucose level and glucose tolerance[2], but it is difficult to cure fundamentally when these indexes are abnormal[3]. A new technique for the early diagnosis of T2DM is very important and strongly desired. T2DM is associated with functional loss of the β-cell mass (BCM), and a BCM decrease occurs before the appearance of clinical symptoms of T2DM[4]. Therefore, the BCM in the pancreas is believed to be a promising biomarker for the early-phase diagnosis and prognosis of diabetes patients.

Amyloid deposition in pancreatic islets, islet amyloid, is one of the most common pathologic features of T2DM, being found in more than 90% of patients at autopsy[5]. Islet amyloid deposits are formed from islet amyloid polypeptide (IAPP), also known as amylin, which is composed of 37 amino acids[6]. Islet amyloid formation is closely associated with a reduced BCM in diabetic patients[7]. A previous study also reported that islet amyloid deposition precedes the onset of hyperglycemia in monkeys[7]. Taken together, these findings suggest a close relationship between islet amyloid deposition and the development and progression of T2DM[7].

Amyloid is a generic term for a specific protein aggregation state characterized by β-sheet conformation. In humans, more than 20 proteins are known to create amyloid fibrils[8]. β-amyloid (Aβ), which accumulates in the brains of Alzheimer's disease (AD) patients, is one of the most well-known amyloids and is widely considered one of the causative factors of AD[9,10]. Consequently, in vivo imaging of Aβ plaques with noninvasive techniques, such as positron emission tomography (PET) or single photon emission computed tomography (SPECT), is expected to be useful for the presymptomatic diagnosis of AD, and many PET and SPECT probes for Aβ imaging have been developed[11,12]. Since Aβ imaging probes are designed to bind to β-sheet conformations in aggregates, they are likely to bind to not only Aβ aggregates but also other amyloid aggregates. A previous report demonstrated that [^{11}C]PiB, the golden standard of Aβ imaging tracers, could visualize myocardial amyloid deposits in patients diagnosed with systemic amyloidosis[13]. Based on the previous findings, we considered that Aβ imaging probes could be applied for the in vivo imaging of amylin aggregates for the prognosis and early diagnosis of T2DM patients. There have been no reports regarding the development of such amylin imaging probes, while some fluorescence probes including thioflavin-T or S (ThT or ThS) and Congo Red, which are commonly used as amyloid dyes, were reported to be able to stain areas of islet amyloid deposition[14]. Recently, we reported that one
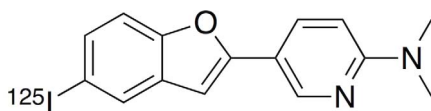
Figure 1 | Chemical structure of [125I]IPBF.

of our Aβ imaging probes, [125I]IPBF (Figure 1), exhibited high binding affinity for Aβ aggregates to visualize Aβ plaques in vivo[15]. In the present study, we investigated the feasibility of amylin imaging in the T2DM pancreas using [125I]IPBF as one of the model compounds of Aβ imaging probes.

Results

[125I]IPBF exhibits high binding affinity for amylin aggregates. To determine the binding affinity of [125I]IPBF to amylin aggregates, we prepared [125I]IPBF[15] (Figure S1 in Supplementary information) and carried out saturation binding assays using amylin aggregates. The saturation curve of [125I]IPBF is shown in Figure 2. Scatchard analysis revealed that [125I]IPBF has a high binding affinity for not only Aβ aggregates but also amylin aggregates ($K_d = 8.31 \pm 1.24$ nM, $B_{max} = 7,130 \pm 943$ pmol/mg protein).

Comparison of binding affinity for amylin aggregates by inhibition experiments. To compare the binding affinity of [125I]IPBF to amylin aggregates with the other Aβ imaging probes reported previously, we conducted in vitro inhibition experiments using [125I]IPBF as the competing ligand. Several Aβ imaging probes with satisfactory binding properties for fibrils, including pyridylbenzofuran derivatives (IPBF[15] and FPYBF-1[16]), an arylquinoxaline derivative (PQ-6)[17], 6-iodo-2-(4-N,N-dimethylamino)-phenylimidazo [1,2-a]pyridine (IMPY)[18], and (E)-4-(2-(6-(2-(2-(2-fluoroethoxy)ethoxy)ethoxy)pyridin-3-yl)vinyl)-N-methylaniline (AV-45, Florbetapir)[19], were chosen as the test compounds (Figure 3). The results are shown in Table 1. All test compounds inhibited the binding of [125I]IPBF to amylin aggregates at K_i values ranging from 2.66 to 501 nM. As a result, among the 6 compounds, IPBF showed the highest affinity for amylin aggregates, with a K_i value of 2.66 ± 0.554 nM.

Structure-activity relationships of IPBF. To determine the factors involved in the high binding affinity of IPBF and optimize its structure, we compared the affinities (K_i in inhibition experiments) of four benzofuran derivatives whose structures closely resembled IPBF, including two more novel benzofuran derivatives (Figure 4 and Chemistry section in Supplementary information). The results are shown in Table 2. Among the 4 compounds, IPBF exhibited the highest affinity for amylin aggregates. Deletion of the dimethylamino group (IPBF-1) decreased the affinity. This suggests that the dimethylamino group is essential for binding to amylin aggregates. Although the deletion of iodine (PBF) also decreased
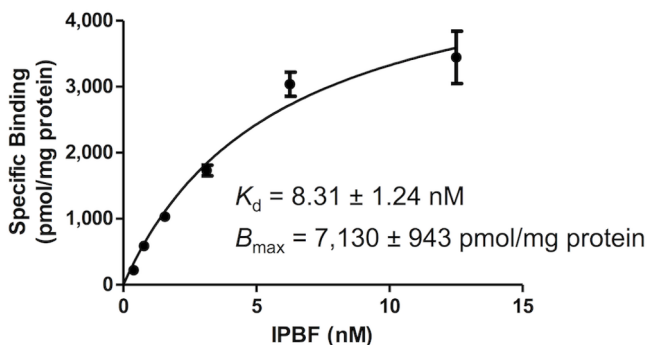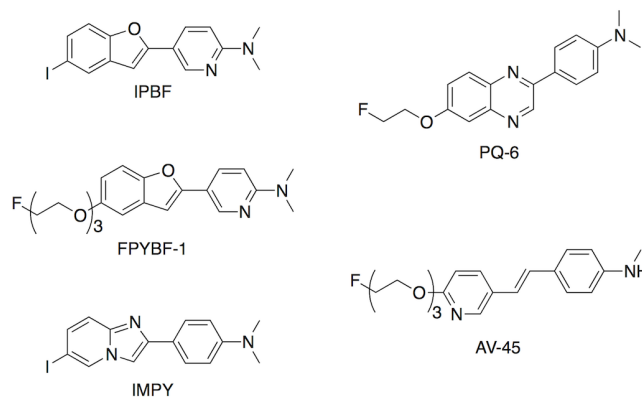
Figure 3 | Chemical structure of previously reported Aβ imaging probes.

the affinity, the level of decrease was much less than the deletion of the dimethylamino group. In contrast, replacement of iodine by a fluoropegylated group (FPYBF-1) did not markedly affect the affinity, suggesting that the replacement of iodine may be acceptable, although the substituted group at position 5 in the benzofuran scaffold is related to binding to some extent. Considering the binding properties in vitro, we selected [125I]IPBF for further characterization as an amylin imaging probe.

[125I]IPBF demonstrates binding to islet amyloids in sections of human pancreas tissue. [125I]IPBF was investigated to assess whether it exhibited selective binding to amylin by autoradiography in human pancreas sections. An autoradiographic image of [125I]IPBF showed the intensive accumulation of radioactivity in the T2DM pancreatic section (Figure 5A), while there was less or no accumulation in healthy control pancreatic sections (Figures 5D and 5G). Each accumulation in the pancreatic sections of T2DM and the healthy controls corresponded with the results of the fluorescence image with ThS in the same section, respectively (Figures 5B, 5E, and 5H). The existence of amylin in these sections was confirmed by immunohistochemical staining with rabbit amylin polyclonal antibody (Figures 5C, 5F, and 5I). In the T2DM pancreatic section, the accumulation of [125I]IPBF was mostly consistent with amylin immunostaining (Figures 5A and 5C). In the older healthy control pancreatic section (71-year-old man), the accumulation of [125I]IPBF was consistent with some of the positive areas on amylin immunostaining (Figures 5D and 5F). These areas were also positive on ThS staining (Figures 5E and 5F). Conversely, there was no specific accumulation of [125I]IPBF in the younger healthy control pancreatic section (28-year-old man) (Figure 5G). Although abundant amylin existed in this pancreatic tissue section (Figure 5I), it showed no amyloid aggregates stained with ThS (Figure 5H). We also stained the sections with anti Aβ$_{1-40}$ and Aβ$_{1-42}$ monoclonal antibodies. They did not show marked 3,3'-diaminobenzidine (DAB) signals in the T2DM patient sections (Figures 5J and 5K), while a series of Aβ in AD brain sections were stained positive for these antibodies (Figure S2 in Supplementary information).

Figure 2 | Saturation curve of [125I]IPBF for amylin aggregates.

$K_d = 8.31 \pm 1.24$ nM

$B_{max} = 7,130 \pm 943$ pmol/mg protein

Table 1 | Comparison of Binding Affinity of Previously Reported Aβ Imaging Probes for Amylin Aggregates

Compound	K_i (nM)*
IPBF	2.66 ± 0.554
FPYBF-1	12.5 ± 1.67
IMPY	71.8 ± 10.1
PQ-6	61.4 ± 8.75
AV-45	501 ± 40.8

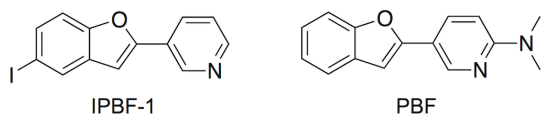*Values are the means ± standard errors of 3-4 independent determinations.

Figure 4 | Chemical structure of pyridylbenzofuran derivatives.

Discussion

We previously reported that [125I]IPBF may be a promising Aβ imaging probe with high binding affinity for Aβ aggregates (K_i = 2.36 nM)[15]. Since most Aβ imaging probes, including IPBF, recognize a β-sheet secondary structure in aggregates, we hypothesized that there is a strong possibility they can also bind to other β-sheet-rich conformers. In the present study, we selected [125I]IPBF as a model compound for Aβ imaging probes and evaluated its potential for amylin imaging.

In the saturation experiment, [125I]IPBF showed a high binding affinity for amylin aggregates (K_d = 8.31 nM) that satisfied one of the criteria required for amylin imaging radiotracers (Figure 2). Furthermore, IPBF displayed a higher binding affinity for amylin aggregates than the other Aβ imaging probes (Table 1). AV-45, which was approved by the FDA for clinical AD diagnosis, displayed a low affinity for amylin (K_i = 501 nM), but a high affinity for AD brain samples (K_i = 6.7 nM)[20]. These results suggest that the binding mode may be slightly different between amylin and Aβ, while they share common β-pleated sheets.

In vitro autoradiography experiments demonstrated that [125I]IPBF binds to islet amyloids in human pancreatic tissue from T2DM patients (Figure 5A). However, [125I]IPBF showed no marked radioactivity accumulation in the pancreatic tissue section from the younger healthy control (Figure 5G), although it exhibited slight accumulation in pancreatic tissue section from the older healthy control (Figure 5D). Considering that its accumulation was consistent with ThS histofluorescence staining, [125I]IPBF seemed to bind to islet amyloids in the normal aging pancreas. It has been reported that islet amyloid also occurs in non-diabetic elderly people, although the amount and frequency are less than in age-matched T2DM patients[21]. It is controversial whether islet amyloidosis is a normal aging phenomenon which is accelerated in T2DM, or whether non-diabetic individuals with islet amyloids are in the process of developing the disease[21]. Therefore, our findings from in vitro autoradiography experiments suggest that in vivo amylin imaging may generate some false-positive results in T2DM diagnosis, while it showed the possibility of the early detection of T2DM. To clarify the relationship between islet amyloid deposition and the onset of T2DM, long-term clinical studies using amylin imaging will be essential in the future.

In the younger healthy control pancreas, [125I]IPBF did not display any specific accumulation, although it included abundant amylin. This was possibly due to a lack of the formation of amyloid aggregates stained with ThS, clearly indicating that [125I]IPBF recognized the β-sheet secondary structure in the islet amyloids, and not the amino acid sequence of amylin. This character of [125I]IPBF should be essential for amylin imaging because native amylin, which is stored in the secretory vesicles in the β-cells, does not form a β-sheet secondary structure[22].

It has been reported that Aβ accumulation occurs in the T2DM pancreas in addition to amylin deposits[23]. Moreover, Aβ was also reported to be co-localized with amylin in islet amyloid deposits[23]. In order to verify the existence of Aβ in islet amyloids, we also conducted immunohistochemical staining with anti-Aβ$_{1-42}$ and anti-Aβ$_{1-40}$ antibodies. As a result, the pancreas tissue sections were totally negative for Aβ$_{1-42}$ and Aβ$_{1-40}$ (Figures 5J and 5K). Taken together, these results suggest that [125I]IPBF bound to amylin in islet amyloid deposits, and not to Aβ. These findings regarding [125I]IPBF strongly indicate that Aβ imaging probes have the potential to func-

Table 2 | Comparison of Binding Affinity of Pyridylbenzofuran Derivatives for Amylin Aggregates

Compound	K_i (nM)*
IPBF	2.66 ± 0.554
FPYBF-1	12.5 ± 1.67
PBF	73.9 ± 5.68
IPBF-1	609 ± 94.9

*Values are the means ± standard errors of 3-4 independent determinations.

tion as amylin imaging probes. This study is the first report on the potential application of Aβ imaging probes to amylin imaging.

For the in vivo imaging of amylin aggregates in the pancreas, it is necessary for imaging tracers to avoid accumulating in organs near the pancreas, such as the liver and intestine. However, Aβ imaging probes, including [125I]IPBF, are designed to exhibit moderate lipophilicity to cross the blood-brain barrier. Small lipophilic molecules are generally inclined to show high initial uptake by the liver, and sequential accumulation in the intestine. A previous study reported that [125I]IPBF exhibited high-level accumulation in the liver and intestine (liver: 31.7 ID%/g at 2 min postinjection, intestine: 50.05 ID%/g at 60 min postinjection)[15]. This characteristic of [125I]IPBF biodistiribution may make it difficult to visualize amylin in islet amyloid deposits in vivo.

The structure-activity relationship study revealed the importance of the dimethylamino group in the pyridylbenzofuran scaffold for binding to amylin aggregates (Table 2). In addition, iodine appeared to be associated with the affinity for amylin aggregates, but the effect of substitution at this position on binding to amylin was low. To decrease the non-specific accumulation of [125I]IPBF in the liver and intestine, it is crucial to enhance the hydrophilicity of compounds to facilitate rapid excretion by the kidney into urine. Based on the results of the structure-activity relationship study, one of the promising structural optimizations of [125I]IPBF is that it is thought to replace iodine, which increases lipophilicity, with hydrophilic substituted groups. Further structural optimization based on [125I]IPBF to reduce its accumulation in organs near the pancreas may lead to a useful tracer for in vivo imaging of islet amyloids in the pancreas.

Methods

Preparation of amylin aggregates. A solid form of amylin was purchased from the Peptide Institute (Osaka, Japan). The peptide was dissolved in DMSO and then diluted with 20 mM Tris/HCl, 100 mM NaCl, pH 7.5 to a final concentration of 100 μM. Aggregation was accomplished immediately after dilution with the buffer.

Saturation binding assay with IPBF using amylin aggregates. A solution of [125I]IPBF (final conc., 0.39–12.5 nM) was prepared by mixing with nonradioactive IPBF. Nonspecific binding was defined in the presence of 200 nM nonradioactive IPBF and 10 mM ThT. One milliliter of the reaction mixture contained 100 μL of [125I]IPBF, including nonradioactive IPBF, 50 μL of amylin aggregates (final conc., 25 nM), and 850 μL of PBS containing 10% DMSO. After incubation for 3 h at room temperature, the binding mixture was filtered through GF/B filters (Whatman, Maidstone, Kent, UK) using an M-24 cell harvester (Brandel Inc., Gauthersburg, MD, USA). Filters containing the bound 125I ligand were counted in a γ counter (Wallac 1470 Wizard; Perkin Elmer, Boston, MA, USA). The dissociation constants (K_d) and B_{max} of IPBF for amylin aggregates were determined by Scatchard analysis using GraphPad Prism 5.0 (Graphpad Software, San Diego, CA, USA).

Competitive inhibition assay with IPBF using amylin aggregates. A mixture containing 50 μL of nonradioactive derivatives in DMSO (final conc., 0.5 pM-25 μM), 50 μL of [125I]IPBF (final conc., 0.025 nM), 50 μL of amylin aggregates (final conc., 25 nM), and 850 μL of PBS containing 10% DMSO was incubated at room temperature for 3 h. The mixture was then filtered through GF/B filters (Whatman) using an M-24 cell harvester (Brandel), and the radioactivity of the filters containing the bound 125I ligand were measured in a γ counter (Wallac 1470 Wizard; Perkin Elmer). Values for the half-maximal inhibitory concentration (IC$_{50}$) were determined from displacement curves using GraphPad Prism 5.0 (GraphPad Software), and those for the inhibition constant (K_i) were calculated using the Cheng-Prusoff equation: K_i = IC$_{50}$/(1 + [L]/K_d), where [L] is the concentration of [125I]IPBF used in the assay and K_d is the dissociation constant of IPBF (8.31 nM).
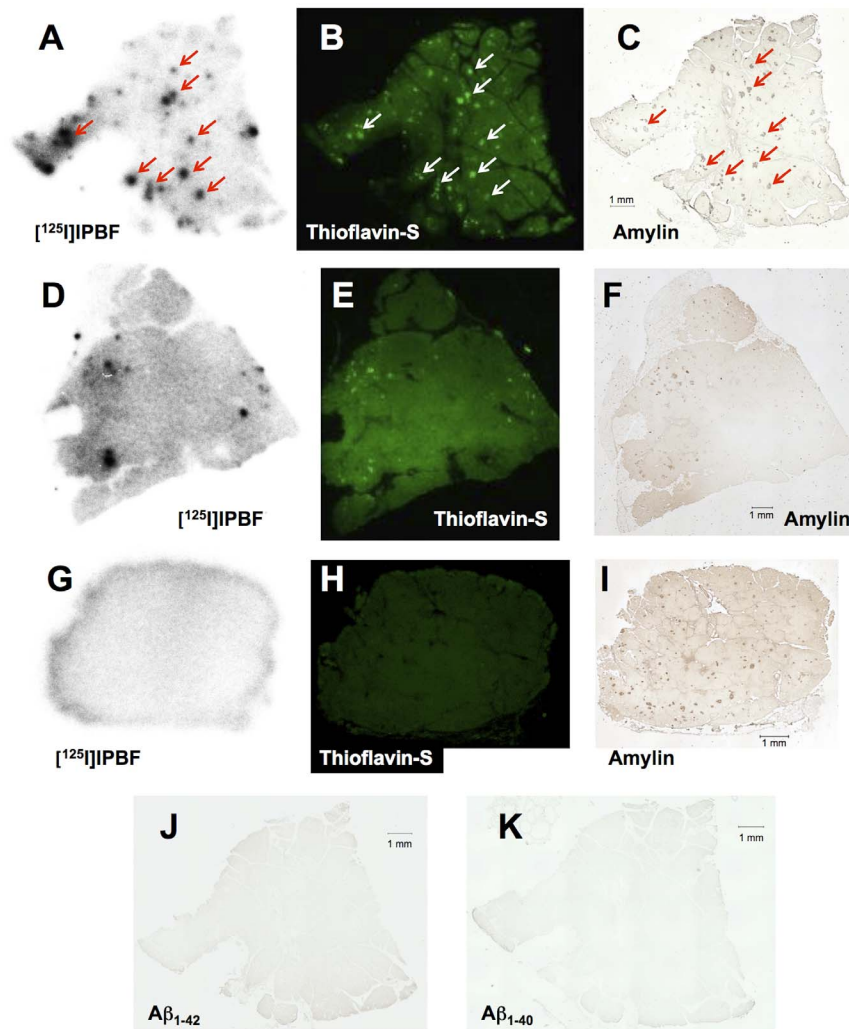
Figure 5 | Comparison of autoradiographic images of [^{125}I]IPBF with pancreatic tissue sections from a T2DM patient and two healthy controls (A, and D and G, respectively). The same sections were also stained with thioflavin-S (B, and E and H, respectively). Immunohistochemical staining with antibodies against amylin (C, and F and I, respectively), Aβ_{1-42} (J), and Aβ_{1-40} (K). Pancreatic tissue sections from a T2DM patient (A, B, C, J, and K) and two different healthy donors (D, E, and F: 71-year-old man; G, H, and I: 28-year-old man).

In vitro **autoradiography using human pancreas sections.** Paraffin-embedded pancreas tissue sections from a T2DM patient (69-year-old woman) and two healthy adults (71-year-old man and 28-year-old man) were purchased from BioChain Institute Inc. (Hayward, CA, USA). The sections were subjected to two 15-min incubations in xylene, two 1-min incubations in 100% EtOH, two 1-min incubations in 90% EtOH, and one 1-min incubation in 70% EtOH to completely deparaffinize them, followed by two 2.5-min washes in water. The sections were incubated with [^{125}I]IPBF (370 kBq/1 mL) for 1 h at room temperature. They were then dipped in 50% EtOH (two 1-min washes) and washed with water (one 30-sec wash). After drying, the ^{125}I-labeled sections were exposed to a BAS imaging plate (Fuji Film, Tokyo, Japan) for 3 h. Autoradiographic images were obtained using a BAS5000 scanner system (Fuji Film).

ThS staining of islet amyloids in human pancreas sections. ThS staining was carried out after the autoradiographic study using the same pancreas tissue sections. The sections were immersed in 100 μM ThS solution containing 50% EtOH and washed with water. After drying, the sections were examined using a microscope (Eclipse 80i; Nikon, Tokyo, Japan) equipped with a BV-2A filter set (excitation, 400–440 nm; dichroic mirror, 455 nm; long-pass barrier filter, 470 nm).

Immunohistochemical staining using human pancreas sections. Paraffin-embedded pancreas tissue sections from a T2DM patient (69-year-old woman) and two healthy adults (71-year-old man and 28-year-old man) were purchased from BioChain Institute Inc. After deparaffinization of the sections according to the same method as described in the *in vitro* autoradiography experiments, they were then autoclaved for 15 min in 0.01 M citric acid buffer (pH 6.0) for antigen retrieval, followed by two 5-min incubations in PBS-Tween20. For the further antigen retrieval of Aβ_{1-40} and Aβ_{1-42}, they were incubated at room temperature with 90% formic acid solution for 5 min for antigen retrieval, followed by washing under

running tap water for 5 min and one 2-min incubation in PBS-Tween20. The sections were incubated with rabbit polyclonal amylin primary antibody, mouse monoclonal Aβ_{1-42} primary antibody, or mouse monoclonal Aβ_{1-40} primary antibody overnight. After three 5-min incubations in PBS-Tween20, they were incubated with biotinylated goat anti-rabbit IgG and biotinylated goat anti-mouse IgG at room temperature for 1.5 h for amylin and Aβ staining, respectively. After three 5-min incubations in PBS-Tween20, the sections were incubated with Streptavidin-Peroxidase complex at room temperature for 1 h. After two 5-min incubations in PBS-Tween20 and one 5-min incubation in TBS, they were incubated with DAB as a chromogen for 5 min. After washing with water, the sections were observed under a microscope (BIOREVO BZ-9000; Keyence Corp., Osaka, Japan).

1. Shaw, J. E., Sicree, R. A. & Zimmet, P. Z. Global estimates of the prevalence of diabetes for 2010 and 2030. *Diabetes Res. Clin. Pract.* **87**, 4–14 (2010).
2. Izucchi, S. E. Clinical practice. Diagnosis of diabetes. *N. Engl. J. Med.* **367**, 542–550 (2012).
3. Buse, J. B. *et al.* How do we define cure of diabetes? *Diabetes Care* **32**, 2133–2135 (2009).
4. Meier, J. J. *et al.* Pancreatic diabetes manifests when beta cell area declines by approximately 65% in humans. *Diabetologia*, **55**, 1346–1354 (2012).
5. Rocken, C., Linke, R. P. & Saeger, W. Immunohistology of islet amyloid polypeptide in diabetes mellitus: semi-quantitative studies in a post-mortem series. *Virchows Arch. A: Pathol. Anat. Histopathol.* **421**, 339–344 (1992).
6. Cooper, G. J. *et al.* Purification and characterization of a peptide from amyloid-rich pancreases of type 2 diabetic patients. *Proc. Natl. Acad. Sci. USA* **84**, 8628–8632 (1987).
7. Marzban, L., Park, K. & Verchere, C. B. Islet amyloid polypeptide and type 2 diabetes. *Exp. Gerontol.* **38**, 347–351 (2003).

8. Westermark, P. Aspects on human amyloid forms and their fibril polypeptides. *FEBES J.* **272**, 5942–5949 (2005).
9. Hardy, J. & Selkoe, D. J. The amyloid hypothesis of Alzheimer's disease: progress and problems on the road to therapeutics. *Science* **297**, 353–356 (2002).
10. Finder, V. H. Alzheimer's disease: a general introduction and pathomechanism. *J. Alzheimer's Dis.* **22 Suppl. 3**, 5–19 (2010).
11. Svedberg, M. M., Rahman, O. & Hall, H. Preclinical studies of potential amyloid binding PET/SPECT ligands in Alzheimer's disease. *Nucl. Med. Biol.* **39**, 484–501 (2012).
12. Rowe, C. C. & Villemagne, V. L. Brain amyloid imaging. *J. Nucl. Med. Technol.* **41**, 11–18 (2013).
13. Antoni, G. *et al.* In vivo visualization of amyloid deposits in the heart with ¹¹C-PIB and PET. *J. Nucl. Med.* **54**, 213–220 (2013).
14. Nilsson, K. P. *et al.* Conjugated polyelectrolytes—Conformation-sensitive optical probes for staining and characterization of amyloid deposits. *Chembiochem* **7**, 1096–1104 (2006).
15. Ono, M. *et al.* Development of novel ¹²³I-labeled pyridyl benzofuran derivatives for SPECT imaging of β-amyloid plaques in Alzheimer's disease. *PLoS One* **8**, e74104 (2013).
16. Ono, M. *et al.* Novel ¹⁸F-labeled benzofuran derivatives with improved properties for positron emission tomography (PET) imaging of β-amyloid plaques in Alzheimer's brains. *J. Med. Chem.* **54**, 2971–2979 (2011).
17. Yoshimura, M. *et al.* Structure-activity relationships and in vivo evaluation of quinoxaline derivatives for PET imaging of β-amyloid plaques. *ACS Med. Chem. Lett.* **4**, 596–600 (2013).
18. Kung, M. P. *et al.* IMPY: an improved thioflavin-T derivative for in vivo labeling of β-amyloid plaques. *Brain Res.* **956**, 202–210 (2002).
19. Choi, S. R. *et al.* Preclinical properties of ¹⁸F-AV-45: a PET agent for Aβ plaques in the brain. *J. Nucl. Med.* **50**, 1887–1894 (2009).
20. Zhang, W. *et al.* F-18 polyethyleneglycol stilbenes as PET imaging agents targeting Aβ aggregates in the brain. *Nucl. Med. Biol.* **32**, 799–809 (2005).
21. Höppener, J. W., Nieuwenhuis, M. G., Vroom, T. M., Ahren, B. & Lips, C. J. Role of islet amyloid in type 2 diabetes mellitus: consequence or cause? *Mol. Cell. Endocrinol.* **197**, 205–212 (2002).
22. Cao, P., Abedini, A. & Raleigh, D. P. Aggregation of islet amyloid polypeptide: from physical chemistry to cell biology. *Curr. Opin. Struct. Biol.* **23**, 82–89 (2013).
23. Miklossy, J. *et al.* Beta amyloid and hyperphosphorylated tau deposits in the pancreas in type 2 diabetes. *Neurobiol. Aging* **31**, 1503–1515 (2010).

Acknowledgments

Author contributions

M.Y., M.O., H.W., H.K. and H.S. designed the study. M.Y. carried out the experiments. M.Y., M.O., H.W., H.K. and H.S. analyzed the data. M.Y. and M.O. wrote the paper. All authors contributed to discussions and manuscript review.

Additional information

Supplementary information accompanies this paper at http://www.nature.com/scientificreports

Competing financial interests: The authors declare no competing financial interests.

How to cite this article: Yoshimura, M., Ono, M., Watanabe, H., Kimura, H. & Saji, H. Feasibility of Amylin Imaging in Pancreatic Islets with β-Amyloid Imaging Probes. *Sci. Rep.* **4**, 6155; DOI:10.1038/srep06155 (2014).